frontiers in Materials

ORIGINAL RESEARCH
published: 22 April 2020
doi: 10.3389/fmats.2020.00087

Lead Free Multilayer Piezoelectric Actuators by Economically New Approach

Fayaz Hussain[1,2], Amir Khesro[1,3], Zhilun Lu[1,4], Ge Wang[1] and Dawei Wang[1]*

[1] Department of Materials Science and Engineering, University of Sheffield, Sheffield, United Kingdom, [2] Department of Materials Engineering, NED University of Engineering and Technology, Karachi, Pakistan, [3] Department of Physics, Abdul Wali Khan University Mardan, Mardan, Pakistan, [4] The Henry Royce Institute, Sir Robert Hadfield Building, Sheffield, United Kingdom

The replacement of lead zirconate titanate ceramics (PZTs), with a lead-oxide (PbO)-free alternative is the subject of intense investigation worldwide. In this research, a cheap reliable methodology for the fabrication of multilayers (MLs) of lead-free potassium sodium niobate (KNN)-based ceramics is presented without the need for vacuuming and/or hot isostatic pressing of the tape. The thickness per active layer was 193 μm and 102 μm for the 10 and 16 layer MLs actuators, respectively. Effective d_{33} (piezoelectric coefficient), effective d_{33}* (electrostrain coefficient), bi-polar strain (S_{max}), max displacement, dielectric constant (ϵ_r) and loss (tanδ) are 2500 pC/N, 4604 pm/V, 0.17%, 2.2 μm, 1812 and 2% at 1 kHz, respectively, where the effective d_{33} or d_{33}* is the total output of all layers together. The ultimate target materials for potential substitution with KNN-based ceramics and MLs are commercial PZT-4 and PZT-8.

Keywords: lead free, multilayer, piezoelectric, actuators, KNN

OPEN ACCESS

Edited by:
Laijun Liu,
Guilin University of Technology, China

Reviewed by:
Jiagang Wu,
Sichuan University, China
Weigang Yang,
University of California, Santa Cruz, United States
Kaixin Song,
Hangzhou Dianzi University, China

****Correspondence:***
Fayaz Hussain
fhussain@neduet.edu.pk;
engrfayazned@gmail.com

Specialty section:
This article was submitted to Ceramics and Glass, a section of the journal Frontiers in Materials

Received: *16 February 2020*
Accepted: *25 March 2020*
Published: *22 April 2020*

Citation:
Hussain F, Khesro A, Lu Z, Wang G and Wang D (2020) Lead Free Multilayer Piezoelectric Actuators by Economically New Approach. Front. Mater. 7:87. doi: 10.3389/fmats.2020.00087

INTRODUCTION

Piezoelectric actuators are used in many applications (Khesro et al., 2016; Murakami et al., 2018a,b; Wang et al., 2018b, 2019a; Lv et al., 2020). Mostly they are based on lead zirconate titanate ceramics (PZTs) (Lin et al., 2008; Wang et al., 2010, 2011, 2012) the lead content of which is considered toxic and not environmentally friendly particularly in the end of use phase. High temperature piezoelectric devices/transducers and piezoelectric nano-generators are desirable for next generation to monitor the health of appliances, equipment and engines used at elevated temperatures (Zhang and Yu, 2011; Lv et al., 2020). Some lead-free multilayers are fabricated by different approaches (Gao et al., 2015, 2019; Koo et al., 2020; Lv et al., 2020). Nonetheless, Zhu et al. claimed best performance transducer made of $0.96(K_{0.48}Na_{0.52})(Nb_{0.95}Sb_{0.05})O_3–0.04Bi_{0.5}(Na_{0.82}K_{0.18})_{0.5}ZrO_3$ (0.96KNNS–0.04BNKZ) lead free complex composition by a novel phase-boundary engineering (NPB) method. In addition to this, Cu-Ag co-fired $(Bi_{0.37}Na_{0.37}Sr_{0.26})TiO_3$ (BNST) were reported with higher inverse-piezoelectricity, as key properties given in the **Table 1** (Koo et al., 2020). As Compared to the electromagnetic actuators; the miniaturized multilayer-piezoelectric-actuators are non-resonant type with large out-put of force at low applied voltages, containing negligible electromagnetic noises and up to sub-nanometer resolutions in displacement (Uchino, 2008; Koji et al., 2010; Gao et al., 2019). Consequently, replacement piezoelectric compositions are sought, a leading candidate of which is potassium sodium niobate (KNN) (Zhang et al., 2013; Ibn-Mohammed et al., 2016;

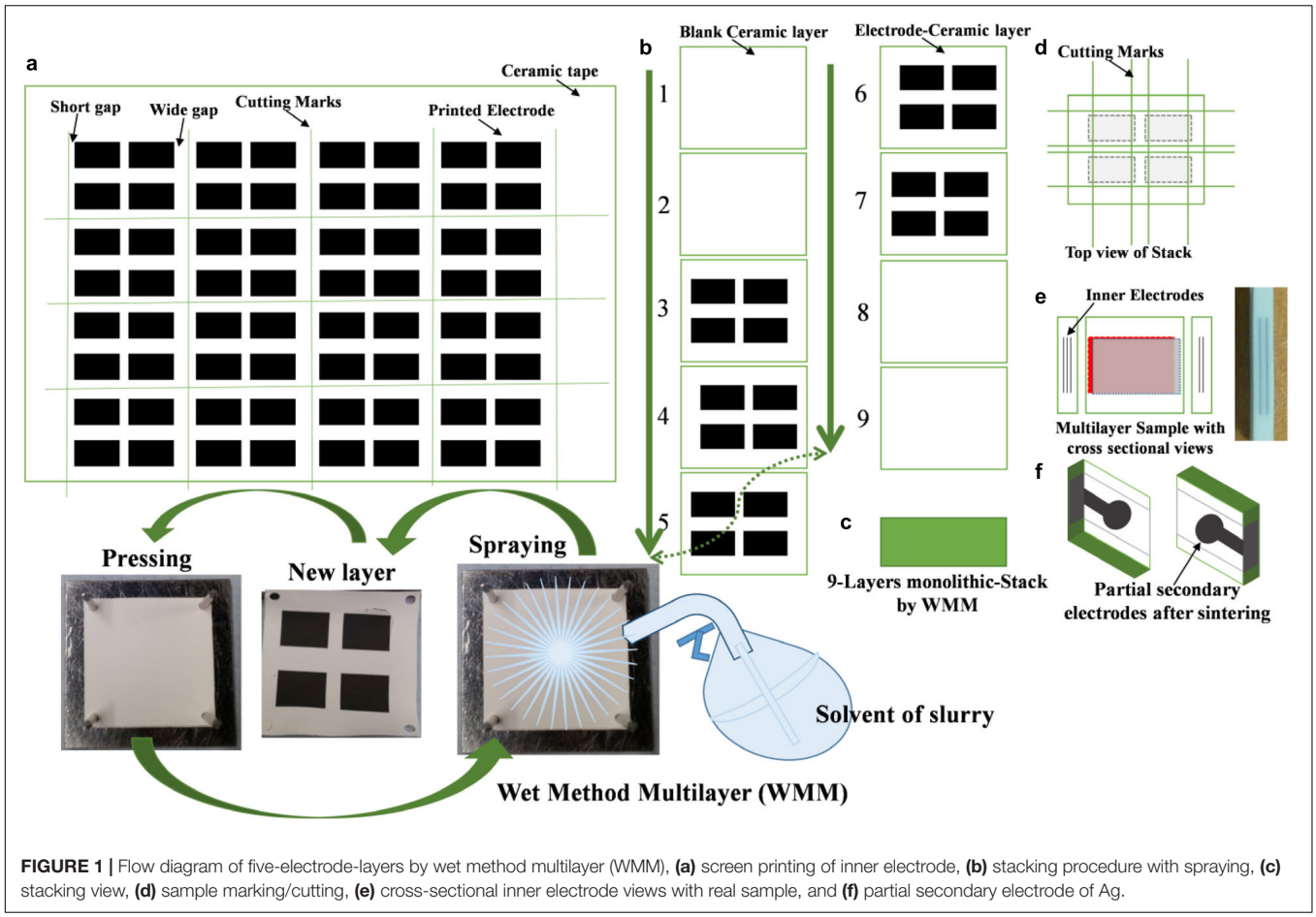

FIGURE 1 | Flow diagram of five-electrode-layers by wet method multilayer (WMM), **(a)** screen printing of inner electrode, **(b)** stacking procedure with spraying, **(c)** stacking view, **(d)** sample marking/cutting, **(e)** cross-sectional inner electrode views with real sample, and **(f)** partial secondary electrode of Ag.

Wang et al., 2016; Yang et al., 2016; Ibn-Mohammed et al., 2017; Hussain et al., 2018, 2019). KNN has the added potential of being safe for deployment as internal medical devices, expanding its potential range of piezoelectric applications to biosensors and internal motors/pumps (Uchino, 2008; Koji et al., 2010; Zhang and Yu, 2011; Gao et al., 2015, 2019; Hussain et al., 2018; Koo et al., 2020).

The main issues of KNN processing were discussed in the other studies, specifically that K_2O and Na_2O are highly volatile (Lee et al., 2008; Lin et al., 2007, 2008; Wang et al., 2008; Tan et al., 2012; Zhao et al., 2013; Bafandeh et al., 2014; Wu et al., 2014; Zheng et al., 2015). However, PbO is also volatile (Donnelly and Randall, 2011) nonetheless PZT is a versatile piezoelectric used commercially, hence it is reasonable to expect this limitation to be overcome in production by adopting similar methodologies to those developed for PZT. The volatility of PbO is known to be sensitive to the incorporation of specific dopants (SrO) and to the Zr:Ti ratio (Zheng et al., 2001, 2002; Reaney, 2007). In KNN based compounds, doping with more stable, less volatile species such as ZrO_2 is considered to inhibit volatilisation (Malic et al., 2008; Hayashi et al., 2012). Moreover, forming solid solutions with $(Na_{1/2}Bi_{1/2})$ ZrO_3 (NBZ) have been shown in other part of this work where different dopants were used to enhance the piezoelectric properties in KNN based formulations (Hussain, 2016; Hussain et al., 2018, 2019). Therefore, from both a processing and properties perspective NBZ with excess ZrO_2 were useful substituents/dopants in KNN. To demonstrate that control of final properties in multilayers could be achieved using low cost raw materials, industrial grade Nb_2O_3 (99.5%) and ZrO_2 (99.0%) were utilized in the fabrication process of some actuators.

Multilayering is a viable, and sustainable technology to optimize properties for many types of functional ceramics (Uchino, 1998; Yao and Zhu, 1998; Kim et al., 2008; Kawada et al., 2009; Erturk and Inman, 2011; Ali et al., 2012; Hayashi et al., 2012; Gao et al., 2014a,b, 2015; Wang et al., 2018a, 2019b, 2020; Li et al., 2019). Typically, multilayers are created by stacking and cutting the samples, vacuuming in plastic bag, hot pressing and/or cold-isostatic pressing (CIP) to adhere the layers prior to firing. In this study, a simple methodology was developed which is heretofore referred to as the wet-method-multilayers (WMM) method which is low cost and simple. The method was developed primarily to resolve issues of delamination which dogged early attempts at multilayering using conventional processing.

It is noted that this study is the first demonstration to the candidate's knowledge of the use of KNN-BNZ in the fabrication of multilayer actuators. Here, the aim was to select the optimum compound to fabricate the MLAs or

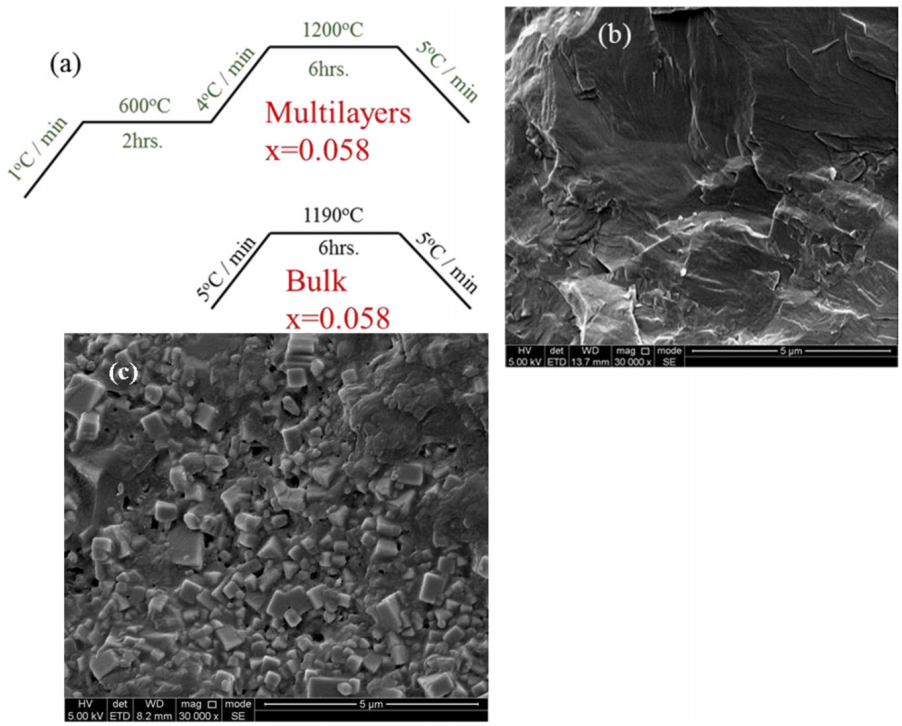

FIGURE 2 | (a) Heat treatment and sintering profile of MLAs and bulk Ceramics, and **(b)** SEM images of fractured surfaces of bulk, and **(c)** single layer of multilayers of (0.942KNN–0.058BNZ) +ZrO_2 ceramics.

TABLE 1 | Comparisons of general properties per layer (bulk) with well-established commercial type piezoelectric Ceramics.

Piezoelectrics	d_{33} (pC/N)	d_{33}* (pm/V)	tanδ	ϵ_r at RT,	T_C (°C)	References
PZT-5A Nvy II	374	374		1700	350	efunda, 2016
PZT-5H Navy IV	593	585		3400	190	efunda, 2016
PZT-4 Navy I		295		1300	325	Wang et al., 1998
PZT-8 Navy III		225		1000	300	Boston Piezo Optics, 2016
KNN-Li (7%)	240	–	0.084	950	460	Hollenstein et al., 2005
NBT-KBT-BT (MPB)	170	–	0.02	730	262	Zang et al., 2007
KNN-CZ 2 (MLCC)	160	360	–	1180	260	Kawada et al., 2009
CuAg/(Bi0.37Na0.37Sr0.26)TiO3	–	575	0.038	2067	<250	Koo et al., 2020
(KNN-0.058BNZ) + ZrO_2 (from Bulk and MLA per layer)	250	423 and 460	0.028 and 0.041 at 1 kHz	1812 and 1750at 1 kHz	300	This Study

[1] *S_{max}, S_{neg}, d_{33}*, d_{33}*(eff) are maximum strain per layer, negative strain per layer, ratio of S_{max} to E_{max} (maximum electric field) or inverse piezoelectric charge coefficient per layer and inverse piezoelectric charge coefficient per all layers, respectively.*

potentially in the future an energy harvester to improve reproducibility by WMM.

MATERIALS AND METHODS

Analytical grade raw materials were used where x = 0.52 (black colored in **Figure 4**) and x = 0.06 (**Figure 4**) in this work; i.e., K_2CO_3 = Fisher Scientific with 99.9% anhydrous, Na_2CO_3 = Fisher Scientific with 99.9% anhydrous, Nb_2O_5 = Stanford Materials Corporations with 99.999%, Bi_2O_3 = Sigma Aldrich with 99.9%, and ZrO_2 = Sigma Aldrich with 99.9%. In addition to this, all other compositions were made of commercial grade powders of Nb_2O_5 = 99.5%, ZrO_2 = 99%, K_2CO_3 = 99.5%, and Na_2CO_3 = 99.5%.

Wet Method Multilayers (WMM): In the WMM method as shown in **Figure 1**, a small quantity of tape-cast solvent was brushed or sprayed onto each layer which could then be laminated by applying a gentle manual pressure. This procedure resolved problems of delamination (**Figure 3**),

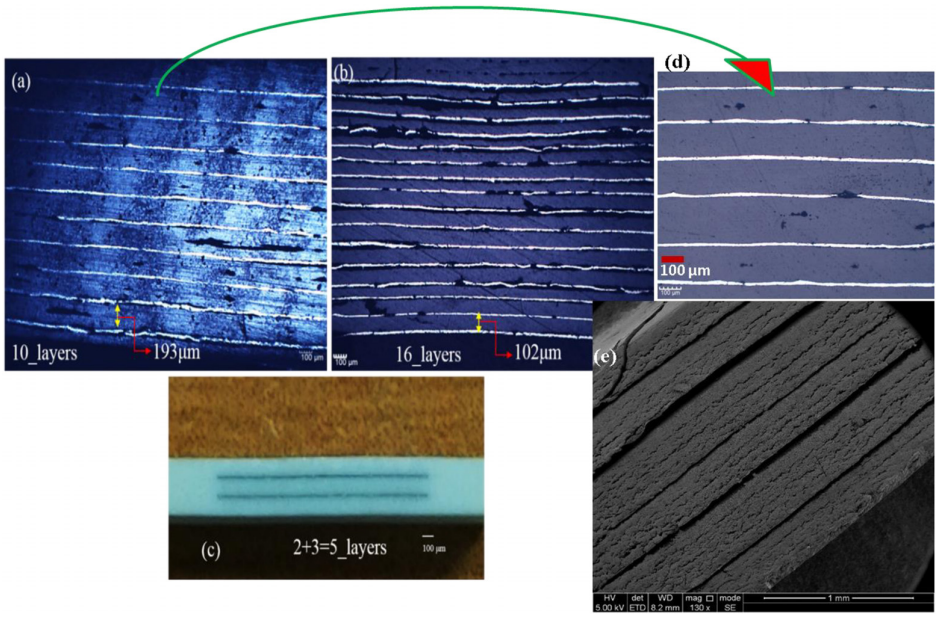

FIGURE 3 | Optical Microscopic viewing cross-sectional images of middle-sectioned sample to show all inner electrodes of **(a)** 10_layers and **(b)** 16_layers MLA (0.942KNN_50/50-0.58BNZ); **(c)** Optical photograph of 5_layers KNN_51/49 showing two alternate layers of inner electrode of one side cross section, **(d)** zooming of 10-layers sample, and **(e)** SEM image (130X) showing severe delamination in conventionally prepared MLAs.

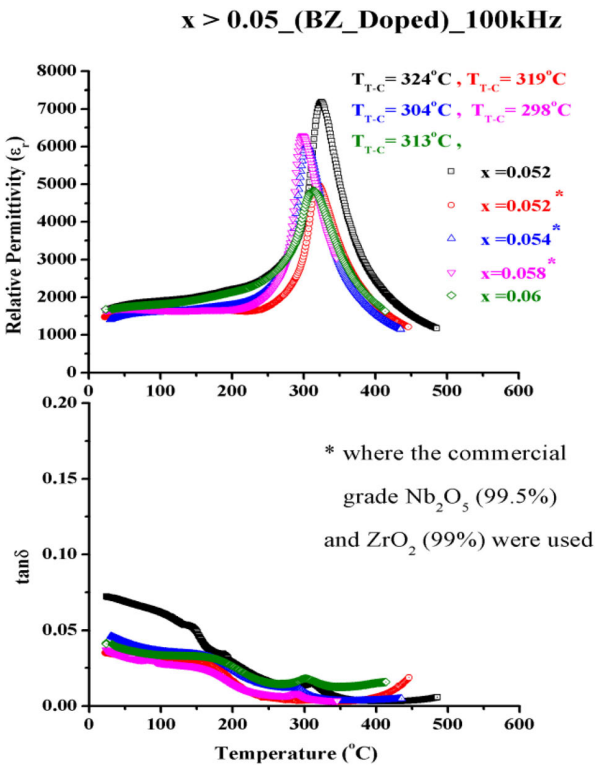

FIGURE 4 | Relative permittivity vs. tanδ loss of BNZ doped where (0.05 ≤ x ≤ 0.06), compared with commercial grade raw materials.

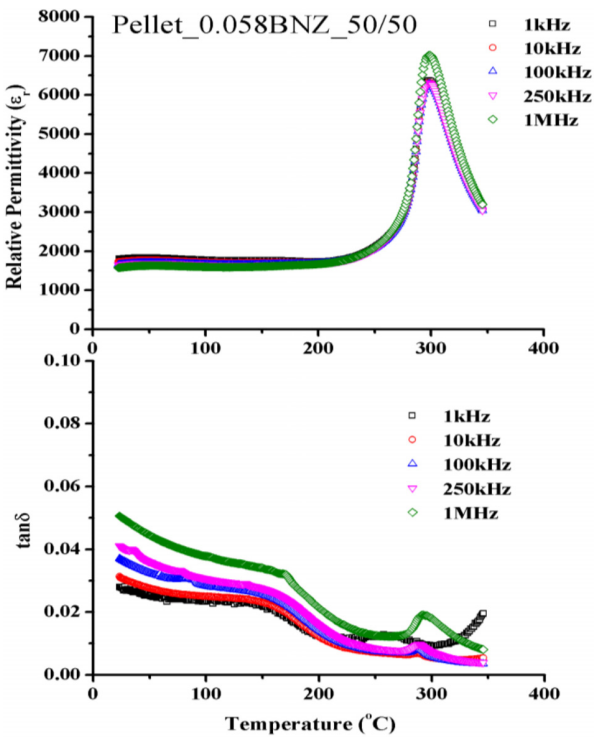

FIGURE 5 | Pellet sample made of commercial grade raw materials of 0.942KNN-0.058BNZ formulation showing relative permittivity and tanδ loss at frequency of 1 kHz–1 MHz.

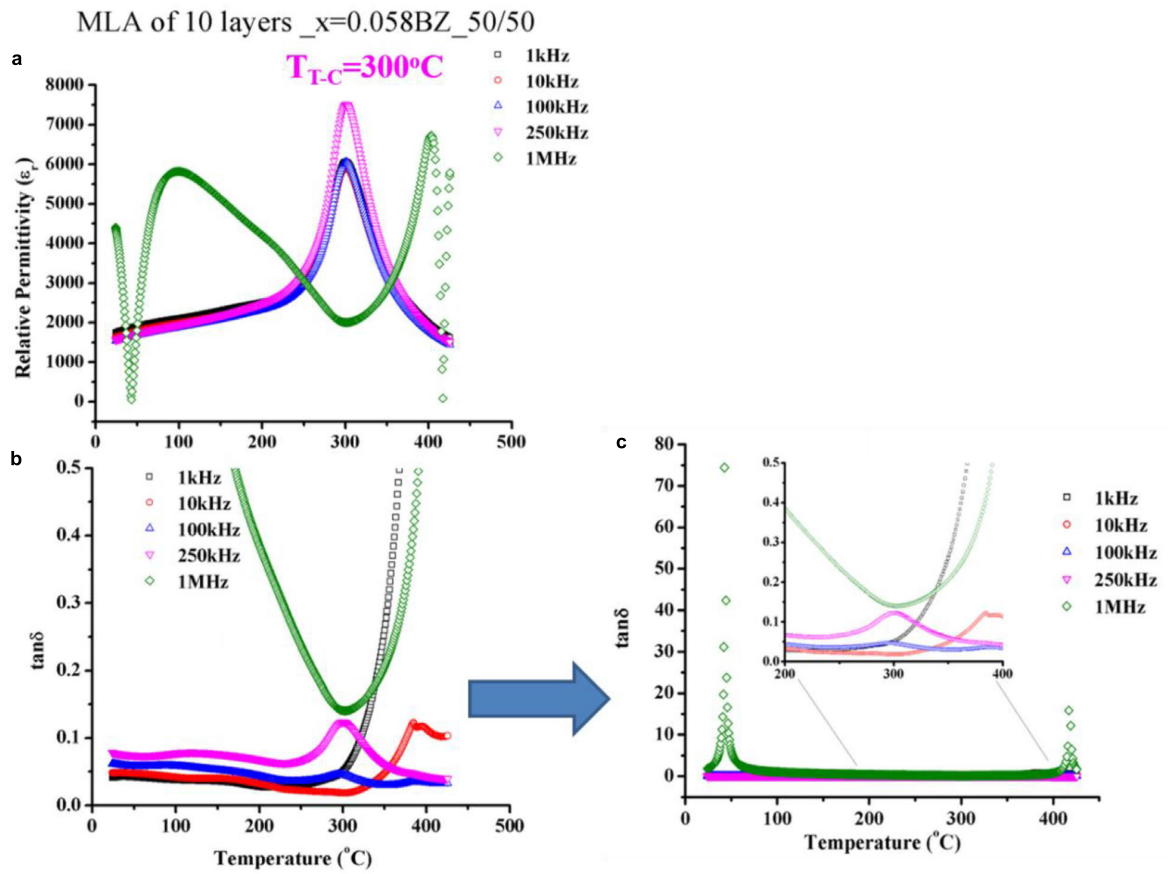

FIGURE 6 | MLA of 10-layers made of commercial grade raw materials of 0.942KNN-0.058BNZ formulation showing **(a)** relative permittivity, **(b)** tanδ loss, and **(c)** tanδ loss of 1 MHz with complete picture.

typically encountered by more conventional lamination methods. Typically, 10–16 layers were pressed together with screen printed Pt electrodes in between. From each stack, four samples were cut with extra green tape then pressed onto the sides of the laminated sample to further minimize delamination (Hussain, 2016).

The disadvantage of standard method is that air between layers of ceramic and electrode may become trapped and cannot be evacuated. During cold isostatic pressing, these air bubbles burst and the liquid of the CIP floods between the layers. If hot pressing is used, it dries the volatiles unevenly and deforms the structure. It is proposed that the WMM method can be modified for potential commercial use with a fine spray mist of the solvent passed over each layer prior to gentle pressure being applied with a rubber pad. The optimized ingredients of recipe of slurry for WMM were ceramic 40 g of powder, 10% of binder butvar, 4% of each PEG and BBP plasticizers, and 50% of isopropanol as a solvent, 0.20% polymeric surfactant (Hypermer KD-1).

The advantage of isopropanol over other solvents (MEK 50%: EtOH 50%) which was used in und-doped KNN on trial basis was that, it evaporated more slowly. But the drawback of isopropanol containing tape was that it needed to be dried at higher temperature (40°C). The slurry was mixed together using high speed mixer (DAC 400 FVZ) at 2000 rpm for 10 min. The ceramic slurry was cast onto the polymeric carrier tape (Mylar carrier substrate) through the doctor blade method (by using table-top tape caster, Mistler TTC-1200) and the tape dried at 40°C for 12-h. The dried green tape was cut into square pieces (30 mm × 30 mm) and patterns were made on the tape using Medway-Cutters (Hussain, 2016) to facilitate screen printing. After screen printing Pt electrodes (9.2 mm × 7.2 mm), multilayer stacks were prepared using a stack-holder (**Figure 1b**) with alternate layers with short and wide gaps. In future, the other electrode-alloy of Ag/Pd could be used, as in the case of $(Na_{0.52}K_{0.44}Li_{0.04})$ $(Nb_{0.89}Sb_{0.05}Ta_{0.06})O_3$ compound was co-fired; but they did not report any functional properties multilayers (Gao et al., 2015). The stacks were carefully withdrawn from the holder and cut into four samples with the help of marking paper (**Figure 1d**). The samples were then placed in a furnace for organic burn off at 600°C with 1°C/min heating rate; and sintered at 1120°C with a heating rate and cooling rate of 4°C/min and 5°C/min, respectively (**Figure 2a**). In addition to this, SEM images are also included in **Figures 2b,c**, **3e** to observe the well sintered samples. After sintering, side of samples (normal to the planar dimensions) were polished to

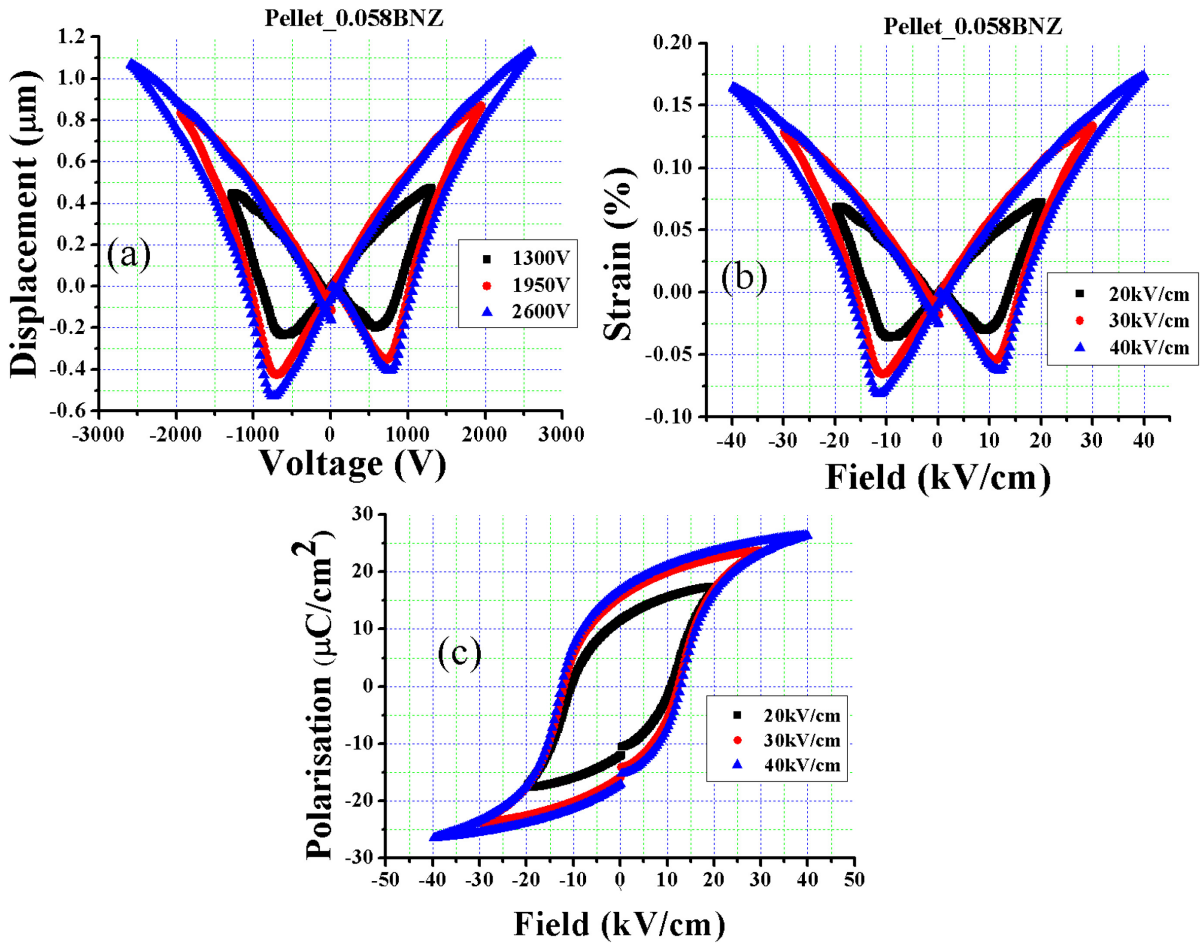

FIGURE 7 | (a) Strain-Voltage, **(b)** Strain-Field, and **(c)** Polarization-Field Hysteresis loops of pellet sample (0.942KNN-0.058BNZ); measured at Sheffield Hallam University.

reveal the inner electrodes and made an electrical connection. Partial surface electrodes (Ag) were pasted and connected to the inner electrodes. The multilayer actuator design is illustrated further in detail in Hussain (2016).

To check the delamination issues, the samples were cut through the center so that all internal Pt electrodes could be observed. Polyvar Met optical microscope with, Carl Zeiss digital camera and Axiovision software was used to take the photos of MLA samples (0.942KNN-0.058BNZ) at 50X magnification, **Figure 3a,b**.

To date, Khesro et al. (2016) (KBT based piezoelectric multilayers) and Nicholls (2016) ($Li_{1/2}Nd_{1/2}TiO_3$ based multilayers) within the Functional Materials and Devices group at Sheffield have been utilised this methodology (WMM) and achieved significantly better densification in their respective multilayers.

The dielectric properties were measured using an LCR meter (Model 4284A, Hewlett Packard). Capacitance and tanδ were measured after every 60 s in a total of 800 scans, from room temperature to 500°C at 1 KHz, 10 KHz, 100 KHz, 250 KHz, and 1 MHz. The samples of MLAs were tested by using the ferroelectric test unit (aix-ACCT TF2000FE-HV Inc., Germany), at "Christian Doppler Laboratory on Advanced Ferroic Oxides," Sheffield Hallam University, Sheffield, United Kingdom. The sample put into silicone oil holder which coupled with a laser-beam-interferometer for recording the displacements in micrometers, where max 40 kV/cm field applied at fixed frequency of 1 Hz to collect the data of P-E and S-E loops at $R_{room\ temperature}$. For poling of the MLAs, the high voltage power supply (Model PS350/5000V – 25W, SRS: Stanford Research Systems, Inc.) used. After that, the Piezometer (Piezotest PM300, PiezoMeter System) was used to measure d_{33} values at a frequency of 110 Hz and at dynamic force of 0.25N.

RESULTS AND DISCUSSION

A SE images of the fracture surfaces of a bulk pellet and MLA are shown in **Figure 2b,c**. Grain boundaries and morphology of grains could not be identified in bulk but partially in MLA even at 30000X magnification, while its relative density was around 98% measured by Archimedes' principle. The high density and

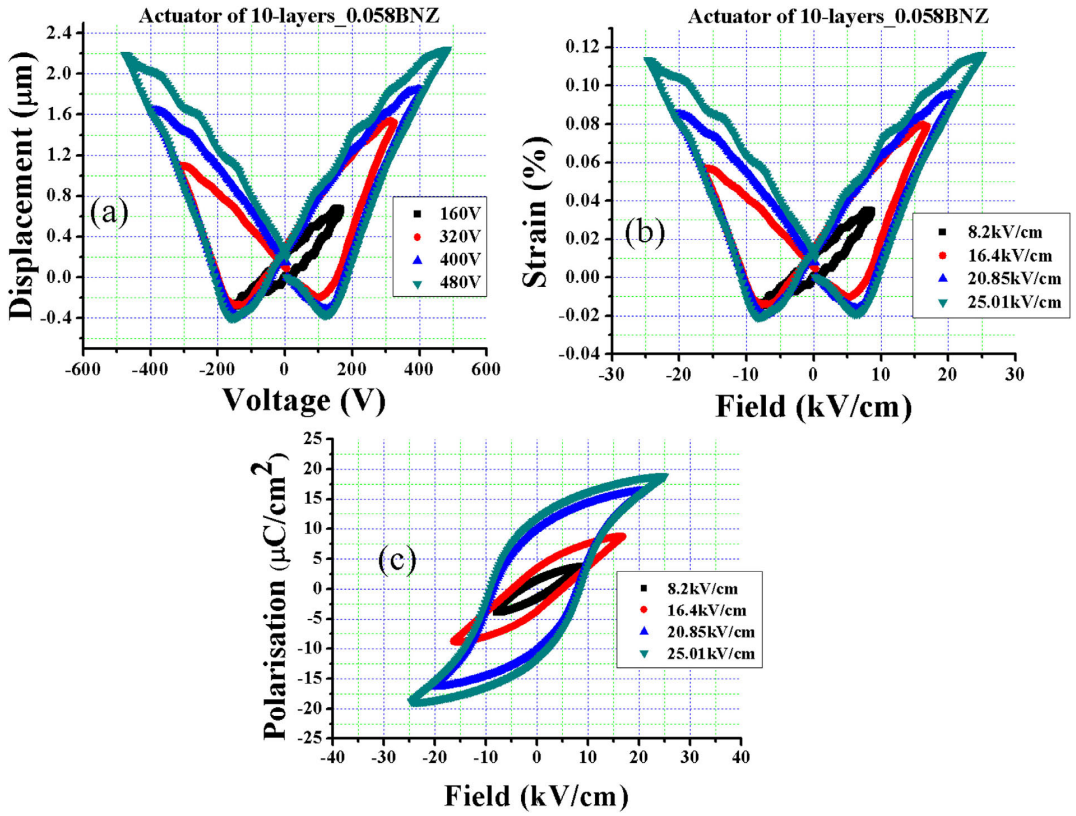

FIGURE 8 | 10-layers MLA sample of (0.942KNN-0.058BNZ) composition showing **(a)** displacement data, **(b)** strain data, and **(c)** ferroelectric loops.

large grain size suggests a liquid phase sintering mechanism but more evidence is required for this to be proved conclusively. The 10 layers are well adhered with a dense ceramic monolithic-layer in between, after heat treatment and sintering (**Figure 3a,d**). After firing, the average thickness of a single layer of ceramic of 10-layers stack sample is 193 μm; approximately double the thickness of the 16-layers sample (i.e., 102 μm).

The greater thickness of the 10 layer sample is because 2 tape cast ceramic layers per electrode layer were utilized whereas the 16 layer sample has only one. The latter was used to minimize the potential of short circuiting during the application of high fields during poling and strain-field measurements. For demonstration, **Figure 3c** shows a 5-layer sample of $K_{0.51}Na_{0.49}NbO_3$ were two electrodes out of 5-layers are clearly visible at one end of the multilayer.

Relative Permittivity and tanδ

ϵ_r and tanδ presented for compositions with $0.06 \geq x \geq 0.05$ (**Figure 4**) and compared at 100 kHz with key formulations also fabricated using commercial grade raw materials of Nb_2O_5 and ZrO_2 to minimize the cost and to improve the overall properties of KNN-BNZ solid solution. The details concerning the dielectric loss of KNN-BNZ compounds, described in previous works (Wang et al., 2014; Hussain, 2016). In general, the higher the percentage of ZrO_2 the lower the dielectric loss as reported (Kahoul et al., 2014).

The exact composition and temperature of the so called MPB in KNN-BNZ varied with processing even if different Na/K ratios were utilized, as discussed in a previous study (Wang et al., 2016; Hussain et al., 2018). For MLAs; hence the KNN-50/50-0.058BNZ+ZrO_2 selected in which the T_{O-T} transition is below RT, as this gave the most reproducible properties despite d_{33} being the highest for x = 0.052 (d_{33} = 315 pC/N) processed using analytical grade raw materials (Zheng et al., 2001).

Consequently, compositions with x = 0.058 were optimized from commercial grade raw materials since at > x = 0.06 ceramics begin to exhibit strong relaxations as discussed by Wang et al. (2014) There is some variation in T_C for the compositions illustrated in **Figure 4**; with x = 0.058 the lowest; due to different grades (analytical and industrial) of raw materials were used as discussed in "Materials and Methods" section The variation in tanδ and ϵ_r as a function of frequency is given in **Figure 4**.

T_{T-C} (298°C) for x = 0.058 is comparable with data reported by other authors (Zhang and Yu, 2011; Stevenson et al., 2015b; Weaver et al., 2015) and similar to PZT-4D (320°C) (Ceramics, 2016). **Table 1** compares T_C and ϵ_r at RT for x = 0.058 with other commercial piezoelectric ceramics. Interestingly, the dielectric losses decreased to 1% with increasing temperature, superior to PZT (Stevenson et al., 2015a).

The LCR data of multilayer ceramics of 0.942KNN-0.058BNZ with 10 Pt-inner electrodes were also recorded (**Figure 6a–c**).

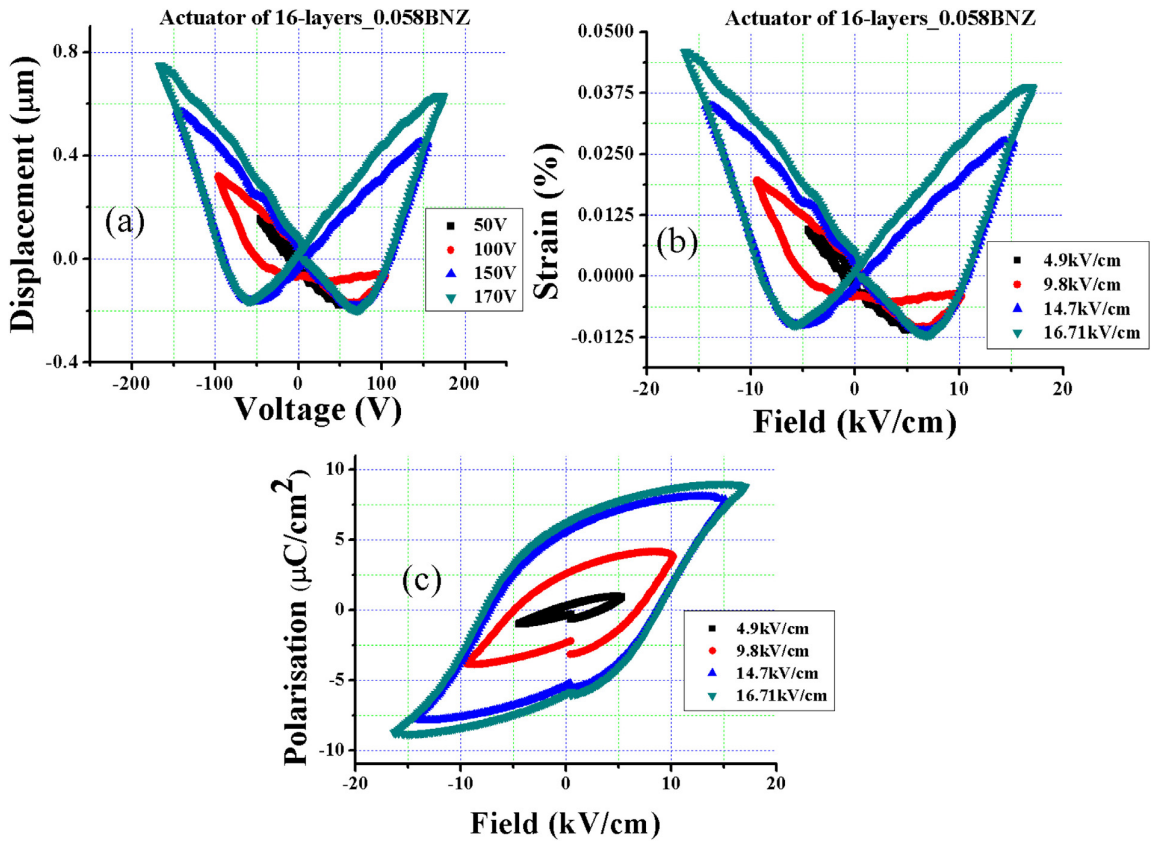

FIGURE 9 | 16-layers MLA sample of 0.942KNN-0.058BNZ compositions showing **(a)** displacement **(b)** strain data, and **(c)** ferroelectric loops.

The dielectric of both the bulk (**Figure 5**) and of the MLA are similar in terms of T_C temperature, ϵ_r and tanδ. However, there is a slope of increasing relative permittivity with increasing temperature from RT in MLA compared to pellet data. There was also a difference in sintering temperatures of bulk (1190°C) and multilayers (1200°C) (**Figure 2**).

It is noted that there is some evidence of resonance modes becoming active in the LCR data presented in **Figure 6a–c**, only at 1 MHz. Whilst this phenomenon is interesting, it is inverse of the polarization peaks at transitions; whereas the peak of this phenomenon is broader at sharper-peak-of-polarization at T_C and vice versa at other points of transitions. Consequently, this resonance behavior is totally opposite to the polarization, and looks more accurate to find the minor changes in the crystalline structure with respect to the temperature at particular resonance frequency.

Ferroelectric Properties of Bulk vs. Multilayers

Strain-voltage, strain-field and polarization-field loops of bulk pellets of x = 0.058 + ZrO_2 (0.76 wt %-age of total ZrO_2) are shown in **Figure 7a–c**, respectively. As discussed previously, ZrO_2 was added to decrease the volatilisation of alkali-ions and therefore the dielectric loss of compositions. Although this is an empirical observation, it is speculated that the extra-addition of Zr^{4+} acts as an acceptor dopant in KNN. Equivalent acceptor doping with Mn and Fe classically controls the dielectric loss in PMN-PT and PZT based ceramics, respectively (Chen et al., 2000; Morozov and Damjanovic, 2008).

The pellet saturated at an applied electric field of 40 kV/cm at room temperature and 1 Hz. All loops are symmetrical and show evidence of ferroelectric/piezoelectric behavior (Kao, 2004). S_{max}, S_{neg}, P_s, P_r, and E_c are 1.1 μm (0.17%),–0.5 μm (0.075%), 26 μC/cm^2, 17 μC/cm^2, and 14.5 kV/cm, respectively, at 40 kV/cm. In general, relaxors do not show negative strain (S_{neg}) and this phenomenon is characteristic of piezoelectric ceramics (Khesro et al., 2016). Both negative and positive strain could be utilized to harvest electrical energy through vibration with the positive mode most effective because it gives rise to greater deflection. The deflection is typically dominated by extrinsic effects which relate to the number and switching behavior of 90° domains walls. 180° are known as ferroelectric domain walls whilst non-180° as the ferroelastic/ferroelectric domain walls (Damjanovic et al., 2005; Reaney, 2007). There has been significant study based on the Rayleigh Law on the behavior of domain walls under applied field in PZT and PbO-free compositions and it is generally accepted that irreversible displacement of non-180° domains is lower in tetragonal compared with rhombohedral compositions (Dragan and Demartin, 1997).

Bulk ceramics are effectively a single thick layer and have limited applications in energy harvesting and related applications. Instead, multilayers are widely used to enhance the properties, performance and reduce the overall cost (Brinkman, 2011).

MLAs with 10 and 16 active layers of (0.942KNN-50/50-0.058BNZ) + ZrO_2 fabricated with Pt inner electrodes were characterized at high field. Strain and P-E loops of the 10-layer (**Figure 8**) MLAs saturated at lower electric field (25 kV/cm) than the pellet (40 kV/cm). Total displacement (2.21 μm/10-layers), S_{max}(0.115%/layer), S_{neg}(0.20 μm/10-layers or 0.010%/layer), d_{33}* (4604 pm/V of 10-layers or 460.4 pm/V per layer), P_s(19 μC/cm^2 per layer), P_r(12 μC/cm^2 per layer), and E_c (8.5 kV/cm per layer) of device are observed, respectively, at 25 kV/cm[1] The low drive field for the MLAs is particularly attractive for applications and in principle, these devices could operate at >200°C since T_C is around 300°C. Nagata et al. (2010) fabricated MLAs based on 0.68($Bi_{0.50}Na_{0.50}$)TiO_3-0.04($Bi_{0.50}Li_{0.50}$)TiO_3-0.28($Bi_{0.50}K_{0.50}$)TiO_3 (BNLKT4-28) and reported d_{33}, S_{max} and displacement of 130 pC/N, 0.17% and 2.1 μm, respectively, at much higher applied electric field (70 kV/cm).

Each active piezoelectric layer in the 16-layer MLA (**Figure 9b** and **Figure 3**) is thinner than that in the 10-layer sample and could only sustain a weaker applied field (16.71 kV/cm) but the properties were similar and more symmetrical to the 10 layer actuators at the same respective electric field. Ferroelectric loops (**Figure 9c**) at this applied voltage were beginning to saturate but higher voltages to achieve full saturation could be applied without breakdown. Images obtained from scrap tape revealed more porosities and delamination in the sintered form than in the 10 layer samples, as shown in **Figure 3b**. The total displacement (**Figure 9a**) of the 16-layer sample was 0.70 μm at relatively low volts (just 170 V) with d_{33}* = 4118 pm/V. It is proposed that when the MLAs are fully optimized, they may be considered as low voltage actuators (≤200 V) (APC, 2010), within the current market.

Table 1 compares commercial PZT with those developed in the present study. The performance of KNN based ceramics are significantly not better than PZT-5H (Navy IV) and similar to PZT-5A (Navy II); but superior to PZT-4 (Navy-I) and PZT-8 (Navy-III). Comparison with other PbO-free ceramics is also shown in **Table 1**.

CONCLUSION

By WMM method, the Lead-free KNN-based MLAs were designed. To control the volatilisation of K and Na, excess Zr^{4+} used which additionally may have acted as an acceptor dopant in the system. At present, 10-layers and 16-layer MLAs with Pt internal electrodes generate 2500 and 3200 pC/N, respectively. Conversely, 10-layer MLAs can actuate with 2.21 μm of displacement at moderately lower applied voltage (480 V); and thin-layers actuator showed promising similar behavior of applied maximum volts (170 V). The effective d_{33}* of 10 and 16 layers were 4604 pm/V and 4118 pm/V, respectively. It is concluded therefore that for other applications such as piezoelectric energy harvesting, KNN-BNZ offers a PbO-free alternative to PZT.

DATA AVAILABILITY STATEMENT

All datasets generated for this study are included in the article/supplementary material.

AUTHOR CONTRIBUTIONS

FH contributed to the investigation, software, data analysis, original draft writing, and critical discussion of results. AK contributed to the formal discussion, review and editing, and conceptualization. ZL contributed to the language, review and editing. GW contributed to the review, editing, and technical additions. DW contributed to the review, editing of the draft, formal analysis, and critical discussion.

FUNDING

FH and AK acknowledge (NED University of Engineering and Technology, Pakistan) and (Abdul Wali Khan University Mardan, Pakistan) for funding support, respectively. All authors acknowledge financial help from the Sustainability and Substitution of Functional Materials and Devices EPSRC grant (EP/L017563/1) through Prof. Ian M. Reaney. ZL wishes to acknowledge the Henry Royce Institute for Advanced Materials, funded through EPSRC grants EP/R00661X/1, EP/S019367/1, EP/P02470X/1, and EP/P025285/1.

ACKNOWLEDGMENTS

We thank "Christian Doppler Laboratory on Advanced-Ferroic-Oxides," Sheffield Hallam University, Sheffield, United Kingdom, for ferroelectric testing. We also thank Dr. Denis Cumming for technical help during screen printing. This work is from Ph.D. thesis of FH (Corresponding Author, Hussain, 2016).

REFERENCES

Ali, H. E., Jiménez, R., Ricote, J., de la Cruz, J. P., Fernandes, J. R. A., and Calzada, M. L. (2012). Properties of multilayer composite thin films based on morphotropic phase boundary Pb($Mg_{1/3}Nb_{2/3}$)O_3-$PbTiO_3$. *Thin Solid Films* 520, 7205–7211. doi: 10.1016/j.tsf.2012.07.118

APC (2010). *First Steps Towards Piezoaction. APC International Ltd.efunda 2016. Lead Zirconate Titanate (PZT-$_5$H)*. Available online at: http://www.efunda.com/materials/piezo/material_data/matdata_output.cfm?Material_ID=PZT-5H (accepted September 09, 2016).

Bafandeh, M. R., Gharahkhani, R., Abbasi, M. H., Saidi, A., Lee, J.-S., and Han, H.-S. (2014). Improvement of piezoelectric and ferroelectric properties in

(K,Na)NbO_3- based ceramics via microwave sintering. *J. Electroceram.* 33, 128–133. doi: 10.1007/s10832-014-9951-z

Boston Piezo Optics (2016). *Ceramic Materials: General Characteristics*. Available online at: http://bostonpiezooptics.com/ceramic-materials-pzt (accepted September 20, 2016).

Brinkman, E. (2011). *The Hidden use of Piezo Technology in Applications all Around us*. Apeldoorn: Stichting Applied Piezo.

Ceramics, M. T. (2016). Available online at: http://www.morgantechnicalceramics.com/en-gb/datasheets/material-datasheets/ (accepted September 16, 2016).

Chen, Y.-H., Hirose, S., Viehland, D., Takahashi, S., and Uchino, K. (2000). Mn-Modified $Pb(Mg_{1/3}Nb_{2/3})O_3$-$PbTiO_3$ ceramics: improved mechanical quality factors for high-power transducer applications. *Japanese J. Appl. Phys. Part 1* 39, 4843–4852. doi: 10.1143/jjap.39.4843

Damjanovic, D., Mayergoyz, I., and Bertotti, G. (eds) (2005). in *Chapter4, 'Hysteresis in Piezoelectric and Ferroelectric Materials' The Science of Hysteresis*, Vol. 3, eds G. Bertotti and I. D. Mayergoyz (Amsterdam: Elsevier).

Donnelly, N. J., and Randall, C. A. (2011). Pb loss in $Pb(Zr,Ti)O_3$ ceramics observed by in situ ionic conductivity measurements. *J. Appl. Phys.* 109:104107. doi: 10.1063/1.3585831

Dragan, D., and Demartin, M. (1997). Contribution of the irreversible displacement of domain walls to piezoelectric effect in Barium Titanate and Lead Zirconate Titanate ceramics. *J. Phys. Condens. Matter* 9, 4943–4953. doi: 10.1088/0953-8984/9/23/018

efunda (2016). *Lead Zirconate Titanate (PZT-5H)*. Available online at: http://www.efunda.com/materials/piezo/material_data/matdata_output.cfm?Material_ID=PZT-5H (accessed September 20, 2016).

Erturk, A., and Inman, D. J. (2011). *Piezoelectric Energy Harvesting*. Hoboken, NJ: John Wiley & Sons.

Gao, R., Chu, X., Huan, Y., Sun, Y., Liu, J., Wang, X., et al. (2014a). A study on (K, Na) NbO_3based multilayer piezoelectric ceramics micro speaker. *Smart Mater. Struct.* 23:105018. doi: 10.1088/0964-1726/23/10/105018

Gao, R., Chu, X., Huan, Y., Wang, X., and Li, L. (2014b). Investigation on co-fired multilayer KNN-based lead-free piezoceramics. *Phys. Stat. Solidi (a)* 211, 2378–2383. doi: 10.1002/pssa.201431156

Gao, R., Chu, X., Huan, Y., Zhong, Z., Wang, X., and Li, L. (2015). Ceramic–electrode inter-diffusion of (K, Na)NbO_3-based multilayer ceramics with $Ag_{0.7}0.7Pd_{0.3}$ electrode. *J. Eur. Ceram. Soc.* 35, 389–392. doi: 10.1039/c5fd00028a

Gao, X., Yang, J., Wu, J., Xin, X., Li, Z., Yuan, X., et al. (2019). Piezoelectric actuators and motors: materials, designs, and applications. *Adv. Mater. Technol.* 5:1900716. doi: 10.1002/admt.201900716

Hayashi, H., Kawada, S., Kimura, M., Nakai, Y., Tabata, T., Shiratsuyu, K., et al. (2012). Reliability of nickel inner electrode lead-free multilayer Piezoelectric ceramics. *Japanese J. Appl. Phys.* 51:09LD01. doi: 10.1143/jjap.51.09ld01

Hollenstein, E., Matthew, D., Damjanovic, D., and Setter, N. (2005). Piezoelectric properties of Li- and Ta-modified $(K_{0.5}Na_{0.5})NbO_3$ ceramics. *Appl. Phys. Lett.* 87:182905. doi: 10.1063/1.2123387

Hussain, F. (2016). *Lead-Free KNN-based Piezoelectric Ceramics in Department of Materials Science and Engineering*. Sheffield, United Kingdom: The University of Sheffield, 154.

Hussain, F., Khesro, A., Muhammad, R., and Wang, D. (2019). Effect of Ta-doping on functional properties of $K_{0.51}Na_{0.49}NbO_3$. *Mater. Res. Express* 6:106309. doi: 10.1088/2053-1591/ab3d49

Hussain, F., Sterianou, I., Khesro, A., Sinclair, D. C., and Reaney, I. M. (2018). *p*-Type/*n*-type behaviour and functional properties of $K_xNa_{(1-x)}NbO_3$ ($0.49 \leq x \leq 0.51$) sintered in air and N_2. *J. Eur. Ceram. Soc.* 38, 3118–3126. doi: 10.1016/j.jeurceramsoc.2018.03.013

Ibn-Mohammed, T., Koh, S. C. L., Reaney, I. M., Acquaye, A., Wang, D., Taylor, S., et al. (2016). Integrated hybrid life cycle assessment and supply chain environmental profile evaluations of lead based (lead zirconate titanate) versus lead-free (potassium sodium niobate) piezoelectric ceramics. *Energy Environ. Sci.* 9, 3495–3520. doi: 10.1039/c6ee02429g

Ibn-Mohammed, T., Koh, S. C. L., Reaney, I. M., Sinclair, D. C., Mustapha, K. B., Acquaye, A., et al. (2017). Are lead-free piezoelectrics more environmentally friendly? *MRS Commun.* 7, 1–7. doi: 10.1557/mrc.2017.10

Kahoul, F., Hamzioui, L., and Boutarfaia, A. (2014). The influence of Zr/Ti content on the morphotropic phase boundary and on the properties of PZT–SFN piezoelectric ceramics. *Energy Proc.* 50, 87–96. doi: 10.1016/j.egypro.2014.06.011

Kao, K.-C. (2004). *Dielectric Phenomena in Solids: With Emphasis on Physical Concepts of Electronic Processes, USA*. Cambridge, MA: Academic Press.

Kawada, S., Kimura, M., Higuchi, Y., and Takagi, H. (2009). $(K_{0.5},Na_{0.5})NbO_3$-based multilayer piezoelectric ceramics with nickel inner electrodes. *Appl. Phys. Express* 2:111401. doi: 10.1143/apex.2.111401

Khesro, A., Wang, D., Hussain, F., Sinclair, D. C., Feteira, A., and Reaney, I. M. (2016). Temperature stable and fatigue resistant lead-free ceramics for actuators. *Appl. Phys. Lett.* 109:142907. doi: 10.1063/1.4964411

Kim, M.-S., Jeon, S., Lee, D.-S., Jeong, S., and Song, J.-S. (2008). Lead-free NKN-5LT piezoelectric materials for multilayer ceramic actuator. *J. Electroceram.* 23, 372–375. doi: 10.1007/s10832-008-9470-x

Koji, K., Makoto, O., and Kunihiko, Y. (2010). *Multilayer Piezoelectric Devices and Method of Producing the Same*. Munich: European patent specification.

Koo, B.-K., Lim, D.-H., Saleem, M., Kim, M.-S., Kim, I.-S., and Jeong, S.-J. (2020). Stability of co-fired CuAg/$(Bi_{0.37}Na_{0.37}Sr_{0.26})TiO_3$ multilayer piezoelectric device. *J. Alloys Compd.* 815:152341. doi: 10.1016/j.jallcom.2019.152341

Lee, Y.-h, Cho, J.-h, Kim, B.-i, and Choi, D.-k (2008). Piezoelectric properties and densification based on control of volatile mass of potassium and sodium in $(K_{0.5}Na_{0.5})$ NbO_3 ceramics. *Japanese J. Appl. Phys.* 47, 4620–4622. doi: 10.1143/jjap.47.4620

Li, W.-B., Zhou, D., Xu, R., Wang, D.-W., Su, J.-Z., Pang, L.-X., et al. (2019). $BaTiO_3$-based multilayers with outstanding energy storage performance for high temperature capacitor applications. *ACS Appl. Energy Mater.* 2, 5499–5506. doi: 10.1021/acsaem.9b00664

Lin, D., Kwok, K. W., and Chan, H. W. L. (2007). Dielectric and piezoelectric properties of $(K_{0.50}Na_{0.50}NbO_3–BaZr_{0.050}Ti_{0.950}O_3)$ lead-free ceramics. *Appl. Phys. Lett.* 91;143513.

Lin, H.-B., Cao, M.-S., Yuan, J., Wang, D., Zhao, Q., and Wang, F.-C. (2008). Enhanced mechanical behavior of lead zirconate titanate piezoelectric composites incorporating zinc oxide nanowhiskers. *Chin. Phys. B* 17, 4323–4327. doi: 10.1088/1674-1056/17/11/060

Lv, X., Zhu, J., Xiao, D., Zhang, X., and Wu, J. (2020). Emerging new phase boundary in potassium sodium-niobate based ceramics. *Chem. Soc. Rev.* 49, 671–707. doi: 10.1039/c9cs00432g

Malic, B., Bernard, J., Bencan, A., and Kosec, M. (2008). Influence of zirconia addition on the microstructure of $K_{0.50}Na_{0.50}NbO_3$ ceramics. *J. Eur. Ceram. Soc.* 28, 1191–1196. doi: 10.1016/j.jeurceramsoc.2007.11.004

Morozov, M. I., and Damjanovic, D. (2008). Hardening-softening transition in Fe-doped Pb(Zr,Ti)O[sub 3] ceramics and evolution of the third harmonic of the polarization response. *J. Appl. Phys.* 104:034107. doi: 10.1063/1.2963704

Murakami, S., Ahmed, N. T. A. F., Wang, D., Feteira, A., Sinclaira, D. C., and Reaney, I. M. (2018a). Optimising dopants and properties in $BiMeO_3$ (Me = Al, Ga, Sc, Y, $Mg_{2/3}Nb_{1/3}$, $Zn_{2/3}Nb_{1/3}$, $Zn_{1/2}Ti_{1/2}$) lead-free $BaTiO_3$-$BiFeO_3$ based ceramics for actuator applications. *J. the Eur. Ceram. Soc.* 38, 4220–4231. doi: 10.1016/j.jeurceramsoc.2018.05.019

Murakami, S., Wang, D., Mostaed, A., Khesro, A., Feteira, A., Sinclair, D. C., et al. (2018b). High strain (0.4%) $Bi(Mg_{2/3}Nb_{1/3})O_3$-$BaTiO_3$-$BiFeO_3$ lead-free piezoelectric ceramics and multilayers. *J. Am. Ceram. Soc.* 101, 5428–5442.

Nagata, H., Hiruma, Y., and Takenaka, T. (2010). Electric-field-induced strain for $(Bi_{0.50}Na_{0.50})TiO_3$-based lead-free multilayer actuator. *J. Ceram. Soc. Jpn.* 118, 726–730. doi: 10.2109/jcersj2.118.726

Nicholls, S. J. (2016). *High Permittivity Ceramics for Dielectrically Loaded Applications, in Materials Science and Engineering*. Ph.D. thesis, University of Sheffield, Sheffield.

Reaney, I. M. (2007). Octahedral tilting, domain structure and piezoelectricity in perovskites and related ceramics. *J. Electroceram.* 19, 3–10. doi: 10.1007/s10832-007-9041-6

Stevenson, T., Martin, D. G., Cowin, P. I., Blumfield, A., Bell, A. J., Comyn, T. P., et al. (2015a). Piezoelectric materials for high temperature transducers and actuators. *J. Mater. Sci. Mater. Electron.* 26, 9256–9267.

Stevenson, T., Quast, T., Bartl, G., Schmitz-Kempen, T., and Weaver, P. M. (2015b). Surface mapping of field-induced piezoelectric strain at elevated temperature

employing full-field interferometry. *IEEE Trans. Ultrason. Ferroelectr. Freq. Control* 62, 88–96. doi: 10.1109/TUFFC.2014.006683

Tan, C. K. I., Yao, K., Goh, P. C., and Ma, J. (2012). $0.94(K_{0.50}Na_{0.50})NbO_3$–$0.06LiNbO_3$ piezoelectric ceramics prepared from the solid state reaction modified with polyvinylpyrrolidone (PVP) of different molecular weights. *Ceram. Int.* 38, 2513–2519. doi: 10.1016/j.ceramint.2011.11.021

Uchino, K. (1998). Materials issues in design and performance of piezo actuators:overview. *Acta Metallurg.* 46, 3745–3753. doi: 10.1016/s1359-6454(98)00102-5

Uchino, K. (2008). Piezoelectric actuators 2006. *J. Electroceram.* 20, 301–311.

Wang, D., Cao, M., and Zhang, S. (2011). Piezoelectric ceramics in the $PbSnO_3$-$Pb(Mg_{1/3}Nb_{2/3})O_3$-$PbTiO_3$ ternary system. *J. Am. Ceram. Soc.* 94, 3690–3693. doi: 10.1109/TUFFC.2017.2721443

Wang, D., Cao, M., and Zhang, S. (2012). Piezoelectric properties of $PbHfO_3$-$PbTiO_3$-$Pb(Mg_{1/3}Nb_{2/3})O_3$ ternary ceramics. *Phys. Status Solidi RRL* 6, 135–137. doi: 10.1002/pssr.201206015

Wang, D., Fan, Z., Zhou, D., Khesro, A., Murakami, S., Feteira, A., et al. (2018a). Bismuth ferrite-based lead free ceramics and multilayers with high recoverable energy density. *J. Mater. Chem. A* 6, 4133–4144. doi: 10.1039/c7ta09857j

Wang, D., Fotinich, Y., and Carman, G. P. (1998). Influence of temperature on the electromechanical and fatigue behavior of piezoelectric ceramics. *J. Appl. Phys.* 83:5342. doi: 10.1063/1.367362

Wang, D., Hussain, F., Khesro, A., Feteira, A., Tian, Y., Zhao, Q., et al. (2016). Composition and temperature dependence of piezoelectricity in $(1-x)(K_{1-y}Na_y)NbO_{3-x}(Bi_{1/2}Na_{1/2})ZrO_3$ lead-free ceramics. *Am. Ceram. Soc.* 100, 627–637. doi: 10.1111/jace.14589

Wang, D., Jin, H., Yuan, J., Wen, B., Zhao, Q., Zhang, D., et al. (2010). Mechanical reinforcement and piezoelectric properties of PZT ceramics embedded with nano-crystalline. *Chin. Phys. Lett.* 27:047701. doi: 10.1088/0256-307x/27/4/047701

Wang, D., Wang, G., Murakami, S., Fan, Z., Feteira, A., Zhou, D., et al. (2018b). $BiFeO_3$-$BaTiO_3$: a new generation of lead-free electroceramics. *J. Adv. Dielectr.* 8:1830004. doi: 10.1142/s2010135x18300049

Wang, G., Fan, Z., Murakami, S., Lu, Z., Hall, D. A., Sinclair, D. C., et al. (2019a). Origin of the large electrostrain in $BiFeO_3$-$BaTiO_3$ based lead-free ceramics. *J. Mater. Chem. A* 7, 21254–21263. doi: 10.1039/c9ta07904a

Wang, G., Li, J., Zhang, X., Fan, Z., Yang, F., Feteira, A., et al. (2019b). Ultrahigh energy storage density lead-free multilayers by controlled electrical homogeneity. *Energy Environ. Sci.* 12, 582–588. doi: 10.1039/c8ee03287d

Wang, G., Lu, Z., Li, J., Ji, H., Yang, H., Li, L., et al. (2020). Lead-free $(Ba,Sr)TiO_3$-$BiFeO_3$ multilayer ceramic capacitors with high energy density. *J. Eur. Ceram. Soc.* 40, 1779–1783. doi: 10.1016/j.jeurceramsoc.2019.12.009

Wang, Y., Damjanovic, D., Klein, N., and Setter, N. (2008). High-temperature instability of Li- and Ta-modified $(K,Na)NbO_3$Piezoceramics. *J. Am. Ceram. Soc.* 91, 1962–1970. doi: 10.1111/j.1551-2916.2008.02392.x

Wang, Z., Xiao, D., Wu, J., Xiao, M., Li, F., and Zhu, J. (2014). New lead-free $(1-x)(K_{0.5}Na_{0.5})NbO_{3-x}(Bi_{0.5}Na_{0.5})ZrO_3$Ceramics with high piezoelectricity. *J. Am. Ceram. Soc.* 97, 688–690. doi: 10.1111/jace.12836

Weaver, P. M., Stevenson, T., Quast, T., Bartl, G., Schmitz-Kempen, T., Woolliams, P., et al. (2015). High temperature measurement and characterisation of piezoelectric properties. *J. Mater. Sci. Mater. Electron.* 26, 9268–9278. doi: 10.3390/ma8125456

Wu, J., Wang, X., Cheng, X., Zheng, T., Zhang, B., Xiao, D., et al. (2014). New potassium-sodium niobate lead-free piezoceramic: Giant-d33 vs. sintering temperature. *J. Appl. Phys.* 115:114104. doi: 10.1063/1.4868585

Yang, X., Cheng, Z., Cheng, J., Wang, D., Shi, F., Zheng, G., et al. (2016). Structural and ferroelectric properties of textured KNN thick films prepared by sol-gel methods. *Integr. Ferroelectr.* 176, 171–178. doi: 10.1080/10584587.2016.1252242

Yao, K., and Zhu, W. (1998). Improved preparation procedure and properties for a multilayer piezoelectric thick-film actuator. *Sens. Actuat. A Phys.* 71, 139–143. doi: 10.1016/s0924-4247(98)00162-9

Zang, S., Shrout, T. R., Nagata, H. H., Hiruma, Y., and Takenaka, T. (2007). Piezoelectric properties in $(K_{0.5}Bi_{0.5})TiO_3$-$(Na_{0.5}Bi_{0.5})TiO_3$-$BaTiO_3$ lead-free ceramics. *IEEE Trans. Ultrason. Ferroelectr. Freq. Control.* 54, 910–917.

Zhang, D.-Q., Wang, D.-W., Zhu, H.-B., Yang, X.-Y., Lu, R., Wen, B., et al. (2013). Synthesis and characterization of single-crystalline $(K,Na)NbO_3$ nanorods. *Ceram. Int.* 39, 5931–5935. doi: 10.1016/j.ceramint.2012.11.065

Zhang, S., and Yu, F. (2011). Piezoelectric materials for high temperature sensors. *J. Am. Ceram. Soc.* 94, 3153–3170.

Zhao, Y., Huang, R., Liu, R., Zhou, H., and Zhao, W. (2013). Low-temperature sintering of KNN with excess alkaline elements and the study of its ferroelectric domain structure. *Curr. Appl. Phys.* 13, 2082–2086. doi: 10.1016/j.cap.2013.08.015

Zheng, H., Reaney, I. M., Lee, W. E., Jones, N., and Thomas, H. (2001). Effects of strontium substitution in Nb-doped PZT ceramics. *J. Eur. Ceram. Soc.* 21, 1371–1375. doi: 10.1016/s0955-2219(01)00021-8

Zheng, H., Reaney, I. M., Lee, W. E., Jones, N., and Thomas, H. (2002). Effects of octahedral tilting on the piezoelectric properties of strontium-barium-niobium-doped soft lead zirconate titanate ceramics. *J. Am. Ceram. Soc.* 85, 2337–2344. doi: 10.1111/j.1151-2916.2002.tb00457.x

Zheng, T., Wu, J., Xiao, D., and Zhu, J. (2015). Giant d33 in nonstoichiometric $(K,Na)NbO_3$-based lead-free ceramics. *Scr. Mater.* 94, 25–27. doi: 10.1016/j.scriptamat.2014.09.008

Conflict of Interest: The authors declare that the research was conducted in the absence of any commercial or financial relationships that could be construed as a potential conflict of interest.